

Synthesis and Electrochemistry of Organometallic Cobaltadithiaazulenes

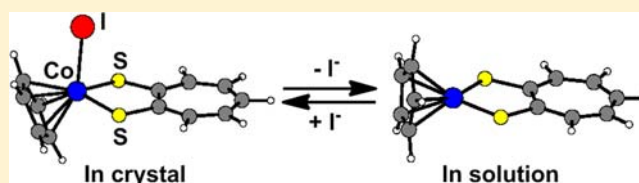
Mitsushiro Nomura,^{*,†} Fumiaki Imamura,[‡] Nguyen Ba Tuyet Nga, Chikako Fujita-Takayama, Toru Sugiyama, and Masatsugu Kajitani^{*}

Department of Materials and Life Sciences, Faculty of Science and Technology, Sophia University, 7-1, Kioi-cho, Chiyoda-ku, Tokyo 102-8554, Japan

Supporting Information

ABSTRACT: Reaction of tropolone or hinokitiol with phosphorus pentasulfide (P_2S_5) directly gives the sulfurized precursor $[PS_2(SST)]_2$ or $[PS_2(SSH)]_2$ (SST = dithiotropolonato or SSH = dithiohinokitiolato). The resulting $[PS_2(SST)]_2$ or $[PS_2(SSH)]_2$ is further reacted with $[CpCoI_2(CO)]$ ($Cp = \eta^5$ -cyclopentadienyl) to form the organometallic $[CpCo(I)(SST)]$ (**1**) or $[CpCo(I)(SSH)]$

(**2**), respectively. **1** and **2** have a cobaltadithiaazulene ring containing one cobalt and two sulfur atoms in the five-membered ring of azulene. Although X-ray structure analysis of **1** reveals the iodide-coordinated structure, **1** becomes the iodide-free complex $[CpCo(SST)]^+$ (4^+) in solution. Electrochemical studies of 4^+ by CV and spectroelectrochemical measurements (ESR, UV–vis–NIR) in solution are carried out. 4^+ is stepwise reduced by $2e^-$ to form the stable neutral radical (4^\bullet) and unstable anion (4^-). It is proposed that the anion 4^- undergoes dimerization to afford the dimer (6^{2-}) by anion radical coupling at the 5 or 7 position in the seven-membered ring of the cobaltadithiaazulene, since the similar anion radical coupling of a reduced azulene has been reported. Electrochemical reoxidation of 6^{2-} slowly undergoes monomerization, giving the original monomer 4^\bullet . DFT calculation of 4^+ explains that there is a delocalized lowest unoccupied molecular orbital (LUMO) in the whole molecule, and that of radical 4^\bullet has a delocalized singly occupied molecular orbital (SOMO). In these $CpCo$ –SST (or SSH) complexes, there could be metal/ligand electron transfer since the SST (or SSH) ligand is potentially redox active. The spin density distribution of 4^- obtained by the DFT method supports the mechanism of the anion radical coupling at the 5 or 7 position in the seven-membered ring.



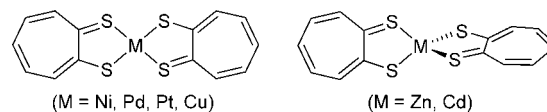
INTRODUCTION

Azulenes are 10π -electron conjugated aromatic compounds and exhibit intramolecular polarization between the five-membered and the seven-membered rings. Application of azulene derivatives is largely because of their unique bicyclic structures containing asymmetric π electrons; thus, an azulene compound has a five-membered cyclopentadienyl anion and a seven-membered tropylium cation. Some of the most notable and useful derivatives of azulene derivatives show near-infrared (NIR) absorption.¹ In addition, azulene derivatives can be also building blocks for potent pharmaceuticals.² Nevertheless, syntheses of azulene compounds containing heteroatoms (heteroazulenes) have been much less investigated than those of substituted azulene derivatives so far. Recently, some other bicyclic compounds (e.g., benzene-fused *N*-heterocyclic carbene (NHCs)) developed by Hahn et al. received much interest based on the important chemical properties.³

In this work, we focused on the syntheses and properties of metalladithiaazulenes, which contain one metal and two sulfur atoms in the five-membered ring of azulene. Holm et al. reported in the 1970s the four-coordinate metal complexes of the bis-dithiotropolonato (SST) ligand, $[M(SST)_2]$ ($M = Ni, Pd, Pt, Cu, Zn,$ and Cd), and their spectroscopic and electrochemical properties.⁴ These metal complexes contain

the bis-metalladithiaazulene rings (Chart 1). The five-membered MS_2C_2 ring in the metal SST complex is nearly

Chart 1. Early Examples of Metalladithiaazulene Compound $[M(SST)_2]^a$



^aSST = dithiotropolonato ligand.

comparable with a metalladithiolenene ring, because these metallacycles show π -electron delocalization. The latter compound, generally so-called ‘metal dithiolenene complex’, has a conjugated system with 6π electrons in the five-membered metalladithiolenene ring. On the basis of the exotic electronic property, the metal dithiolenene complexes have been intensively investigated in many research fields.^{5–8} On the other hand, the metalladithiaazulene may be further conjugated with 10π electrons because there is a π -extended structure with a

Received: May 13, 2012

Published: October 1, 2012

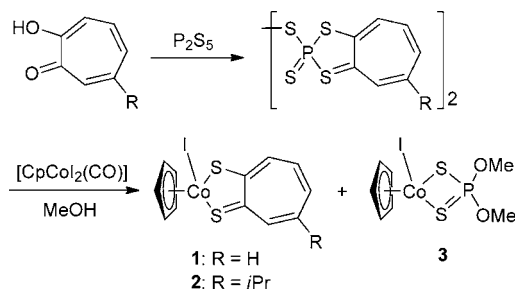
conjugated cycloheptatriene backbone. The first crystal structure of the square-planar $[\text{Ni}(\text{SST})_2]$ complex was reported by Eisenberg et al. in the 1970s.⁹ The bis-nickeladithiaazulene ring is quite planar, suggesting π -electron delocalization. However, since the 1980s, no other works based on the SST complexes or metalladithiaazulene derivatives have been reported so far, although the corresponding oxygen analogues (OOT) and tropolonato derivatives have received much interest for liquid crystalline materials,¹⁰ luminescent materials,¹¹ catalysts in organic reactions,¹² and solvatochromic compounds.¹³

Some reasons for the few reports on the SST derivatives may include difficulties of the synthetic procedure by several reaction steps.⁴ However, in this work, we developed a simple and straightforward procedure to synthesize the organic SST precursor, and it can be also applied for preparation of the analogous dithiohinokitiolato (SSH) precursor. Furthermore, we attempted complexation of the SST or SSH precursor with $[\text{CpCoI}_2(\text{CO})]$ ($\text{Cp} = \eta^5\text{-cyclopentadienyl}$) to synthesize some organometallic cobaltadithiaazulene compounds. Detailed studies on the solution and electrochemical behavior revealed that the organometallic cobaltadithiaazulene compounds showed π -electron delocalization in the whole molecule involving the Cp ligand, generation of a coordinatively unsaturated complex in solution, and an interesting reductive-dimerization based on the seven-membered ring moiety. In order to explain the dimerization reaction mechanism, combined electrochemical and DFT investigations were carried out.

RESULTS AND DISCUSSION

Preparations and Structure Determinations of $[\text{CpCo}(\text{I})(\text{SST})]$ (1) and $[\text{CpCo}(\text{I})(\text{SSH})]$ (2) Complexes. Holm et al. reported that direct sulfurization of tropolone with phosphorus pentasulfide (P_2S_5) alone or in the presence of metal ions did not work to give the dithiotropolonato (SST) derivative or the SST metal complexes at all. The SST derivative was obtained by other reactions in three steps,⁴ although direct sulfurization of benzoin derivatives with P_2S_5 worked well.¹⁴ In this work, however, we found that reaction of tropolone or hinokitiol with P_2S_5 alone in refluxing 1,4-dioxane directly afforded the dithiotropolonato $[\text{PS}_2(\text{SST})]_2$ or dithiohinokitiolato $[\text{PS}_2(\text{SSH})]_2$ derivative in good yield (Scheme 1). Use of fresh P_2S_5 and freshly distilled solvent by Na–benzophenone ensures a higher yield of these products. These isolated $[\text{PS}_2(\text{SST})]_2$ and $[\text{PS}_2(\text{SSH})]_2$ products were further reacted with $[\text{CpCoI}_2(\text{CO})]$ in $\text{CH}_2\text{Cl}_2/\text{MeOH}$ to give $[\text{CpCo}(\text{I})(\text{SST})]$ (1) and $[\text{CpCo}(\text{I})(\text{SSH})]$ (2) in 28% and 44% yields, respectively (Scheme 1). Use of Lawesson's reagent¹⁵ instead of

Scheme 1. Syntheses of $[\text{CpCo}(\text{I})(\text{SST})]$ (1) and $[\text{CpCo}(\text{I})(\text{SSH})]$ (2)



P_2S_5 is also possible, giving the $[\text{PS}_2(\text{SST})]_2$ and $[\text{PS}_2(\text{SSH})]_2$ derivatives and then giving 1 and 2. However, these products were unfortunately obtained in low yields with several unidentified products. 1 and 2 were obtained as air-stable black solids in pure form through filtration from each resulting reaction mixture, whereas 1 and 2 smoothly decomposed when they were exposed to silica gel for chromatographic separation. ^1H NMR spectra of 1 and 2 explained that they were formally diamagnetic with CpCo^{III} oxidation states. In addition to isolation of 1 and 2, one other common product was obtained during preparation. The ^1H NMR spectrum and elemental analysis of the common product indicated a formally diamagnetic CpCo^{III} complex with formula $[\text{CpCo}(\text{I})(\text{S}_2\text{P}(\text{OMe})_2)]$ (3) as shown in Scheme 1. In contrast to 1 and 2, 3 was separated by silica gel column chromatography without any decomposition. The structure of 3 containing a methoxy group explained that MeOH solvent was involved for these reactions.

Complex 1 crystallized in the triclinic system with space group $P\bar{1}$. There are two crystallographically independent molecules (molecules A and B) in the unit cell, but there is no remarkable difference between the two molecular structures. Figure 1 demonstrates the ORTEP drawing for one (A) of the

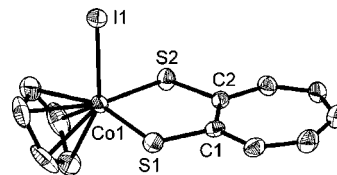


Figure 1. ORTEP drawing of 1. Thermal ellipsoids are drawn at the 30% probability level. One (molecule A) of two crystallographically independent molecules is shown. All hydrogen atoms are omitted for simplicity.

two molecules. Selected bond lengths, bond angles, and dihedral angles are summarized in Table 1. The molecule has a cobaltadithiaazulene ring whose five-membered CoS_2C_2 moiety is fused with a seven-membered cycloheptatriene ring. Although the EI^+ mass spectrum of 1 lacked the iodine atom ($m/z = 277$, $\text{M}^+ - \text{I}$) with the absence of the expected molecular ion peak, X-ray structure analysis of 1 realized that iodide was coordinated to the cobalt and is located in a perpendicular position with respect to the cobaltadithiaazulene ring. Accordingly, this complex is six coordinate with a coordinatively saturated metal center in the solid state. The cobaltadithiaazulene ring is almost exactly planar because of the small deviation from the averaged plane (0.0721 Å). The dihedral angle of Cp/CoS_2 (52.955°) suggests a three-legged piano-stool geometry. The $\text{Co}-\text{I}$ bond length in 1 (2.6507(8) Å for A or 2.6396(8) Å for B) is slightly longer than that of the $[\text{CpCo}(\text{I})(\text{Et}_2\text{dtc})]$ complex (2.597(1) Å), where $\text{Et}_2\text{dtc} = N,N$ -diethyldithiocarbamate.¹⁶ The $\text{Co}-\text{S}$ bond lengths in 1 (2.1928(15) and 2.1835(11) Å) are shorter than those of $[\text{CpCo}(\text{I})(\text{Et}_2\text{dtc})]$ (2.249(1) and 2.255(1) Å)¹⁶ but longer than those of the five-coordinate $[\text{CpCo}^{\text{III}}(\text{dithiolene})]$ complexes (2.10–2.14 Å).¹⁷ This difference of the $\text{Co}-\text{S}$ bond length can be explained by the electronic donation effect of the thiolate ligand on the metal center.¹⁸ Thus, the strong electronic donation effect on the coordinatively unsaturated metal center in the $[\text{CpCo}^{\text{III}}(\text{dithiolene})]$ complexes effectively reduces the $\text{Co}-\text{S}$ bond length.

Table 1. Selected Bond Lengths (Angstroms), Bond Angles (degrees), and Dihedral Angles of [CpCo(I)(SST)] (1), Calculated 1, [CpCo(SST)]ⁿ (4ⁿ, n = -1, 0, +1), and [CpCo(bdt)]ⁿ (n = -1, 0)

	1 ^a	1 ^b	4 ^{+b}	4 ^{*b}	4 ^{-b}	SST ^{-b}	SST ^{*b}	SST ^{+b}	[CpCo(bdt)] ^b	[CpCo(bdt)] ^{-b}
bond lengths										
Co1–S1	2.1928(15)	2.2420	2.1485	2.2050	2.3164				2.1520	2.2333
Co1–S2	2.1835(11)	2.2421	2.1479	2.2050	2.3108				2.1518	2.2348
S1–C1	1.718(4)	1.7271	1.7416	1.7325	1.8254	1.704	1.720	1.754	1.7482	1.7729
S2–C2	1.704(4)	1.7271	1.7420	1.7317	1.8251	1.704	1.720	1.755	1.7482	1.7725
C1–C2	1.425(5)	1.4512	1.4381	1.4575	1.4843	1.501	1.453	1.427	1.4139	1.4166
Co1–I1	2.6507(8)	2.6477								
bond angles										
S1–Co1–S2	88.37(5)	88.64	91.67	90.64	91.07				92.06	91.86
Co1–S1–C1	107.30(16)	106.10	106.00	105.70	104.64				105.18	103.64
Co1–S2–C2	107.44(13)	106.10	106.01	105.72	104.54				105.19	103.67
S1–C1–C2	117.7(3)	119.13	118.17	118.97	119.92	120.68	111.65	101.67	118.78	120.40
S2–C2–C1	119.0(3)	119.13	118.15	118.98	119.82	120.70	111.64	101.64	118.78	120.38
dihedral angle										
Cp/CoS ₂	52.955	53.90	88.97	87.13	89.73				89.29	86.86
CoS ₂ /S ₂ C ₂ ^c	5.58	8.78	0.11	0.17	0.23				0.23	2.00

^aData taken from one of two crystallographically independent molecules. ^bData taken from the optimized structure by the DFT method. ^cCoS₂/S₂C₂ = folding angle along the S··S hinge in the metallacycle.

Figure 2 shows the packing diagram of **1** in the unit cell. We found an alternated π – π stacking such as A··B··A··B along the

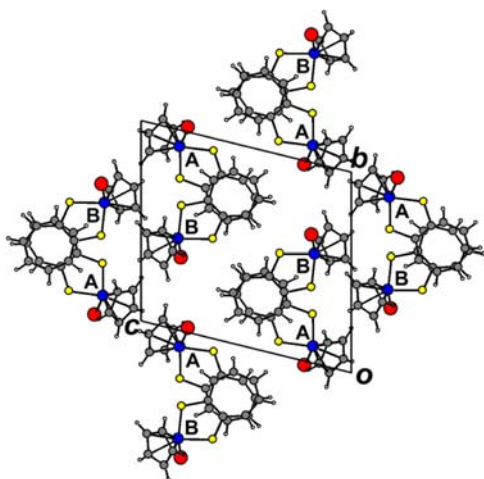


Figure 2. Projection view along the *a* axis of **1** demonstrating an alternated π – π stacking through the seven-membered ring and an intermolecular Cp··Cp face-to-face interaction (Co atom in blue, S atom in yellow, I atom in red, C atom in gray).

a-axis direction based on the seven-membered ring with a distance of ca. 3.5 Å. Liquid crystalline tropolone (OOT) derivatives usually show such molecular stackings.¹⁰ In addition, as an interesting feature of an organometallic complex, there is an intermolecular Cp··Cp face-to-face interaction between two A molecules, but no B molecules are involved for this interaction. Fourmigué et al. and our research group observed several examples of the Cp··Cp interaction in the organometallic [Cp_nM(dithiolene)] (n = 1, M = Co¹⁹ and Ni;²⁰ n = 2, M = W²¹) complexes. When the complexes are paramagnetic, intermolecular magnetic interactions could be realized through the π -orbital overlap of the Cp ligand (e.g., M = Ni and W).

Optimized Structures of 1 and Its Iodide-Free Complexes. As we describe in the following section, **1** and **2** spontaneously eliminate the iodide ligand in solution. Since

the iodide-free complexes [CpCo(SST)]⁺ (4⁺) and [CpCo(SSH)]⁺ (5⁺) were not isolated in this work, we calculated the optimized structure of the closed-shell 4⁺ at the DFT level with the B3LYP method and 6-31G* basis set, as well as **1**, free SST ligand, and [CpCo(bdt)] (bdt = benzene-1,2-dithiolate) for comparison purposes. In order to calculate other open-shell molecules (4^{*}, 4⁻, and [CpCo(bdt)]⁻), we used the UB3LYP method instead. Optimized 4⁺ has a two-legged piano-stool geometry because it can be a five-coordinate half-metallocene complex by elimination of iodide ligand (Figure 3b). In fact, the

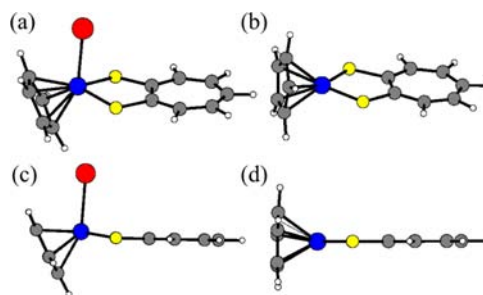


Figure 3. Optimized molecular structures of (a) **1** and (b) the iodide-free complex (4⁺) by DFT calculations. Side views of the molecular structures of (c) **1** and (d) 4⁺ to see the planarity of the cobaltadithiazulene ring (Co atom in blue, S atom in yellow, I atom in red, C atom in gray).

dihedral angle of Cp/CoS₂ in the calculated 4⁺ was 88.97° (Table 1) as a normal two-legged piano-stool structure, whereas the Cp/CoS₂ dihedral angle in calculated **1** was 53.90°, suggesting a three-legged piano-stool geometry (Figure 3a). Although the CoS₂C₂ ring in calculated **1** was slightly folded along the S··S hinge with a folding angle of 8.78° (Table 1 and Figure 3c), the metallacycle of 4⁺ was quite planar (Figure 3d). Furthermore, the Co–S bond lengths of 4⁺ (ca. 2.148 Å) were remarkably shorter than those of **1** (ca. 2.242 Å). This result suggests that a coordinative unsaturation of the cobalt atom in 4⁺ enhances electronic donation of the sulfur atom. In fact, the Co–S bond lengths of 4⁺ were similar to those of the calculated [CpCo(bdt)] (ca. 2.152 Å).²²

One question is the metal–ligand oxidation state in **1** and 4^+ , because the SST (or SSH) ligand may be redox active such as a 1,2-dithiolene ligand. The early paper by Wiegardt et al. reported the X-ray structure of a redox active ligand (*o*-iminobenzosemiquinonate) and its metal complex.²³ They determined the metal–ligand oxidation states by comparing those bond lengths taken from X-ray structure analyses. However, since we did not obtain the X-ray structure of the free SST ligand, we decided to obtain theoretically optimized structures of the SST ligand by DFT methods to compare those oxidation states. The S1–C1, S2–C2, and C1–C2 lengths in the iodinated complex **1** are similar to those of the neutral radical SST $^{\bullet}$ (Table 1). These results suggest that there is Co^{II}–SST $^{\bullet}$ contribution in **1** whereas it is diamagnetic. This is because there could be metal/ligand radicals that are antiferromagnetically coupled since the SST ligand is potentially redox active. Furthermore, the S1–C1, S2–C2, and C1–C2 lengths in the iodide-free complex 4^+ are relatively close to those of the cation SST⁺ (Table 1). Thus, there is probably Co^I–SST⁺ contribution in 4^+ .

We also calculated the optimized structure of the neutral radical (4^{\bullet}), which is formally the $1e^-$ reduced species of 4^+ . Thus, 4^{\bullet} is probably isoelectronic with the $1e^-$ reduced [CpCo(bdt)]⁻. The Co–S bond lengths in 4^{\bullet} (2.205 Å) become longer than those in 4^+ , but they are relatively similar to those in [CpCo(bdt)]⁻ (2.233–2.235 Å) as summarized in Table 1, whereas the fundamental geometry of 4^{\bullet} was comparable with that of 4^+ (Table 1). This result shows that the electronic donation effect of sulfur on the cobalt atom decreases when 4^+ or [CpCo(bdt)] is reduced. The Mulliken atomic spin density analysis by DFT calculation of 4^{\bullet} or [CpCo(bdt)]⁻ indicated that 97% or 100% spin density existed on the central cobalt atom, respectively; thus, there is a large contribution of a reduced Co^{II} state in 4^{\bullet} or [CpCo(bdt)]⁻. It is reasonable that the enhancement of electron density on the Co atom reduces electronic donation of the sulfur atom.

Electrochemical and Solution Behavior of [CpCo(I)(SST)] (1**) and [CpCo(I)(SSH)] (**2**) Complexes.** Cyclic voltammograms (CVs) of **1** and **2** demonstrated in Figure 4b and 4c provided two reduction waves and three oxidation waves in dichloromethane solutions containing tetra-*n*-butylammo-

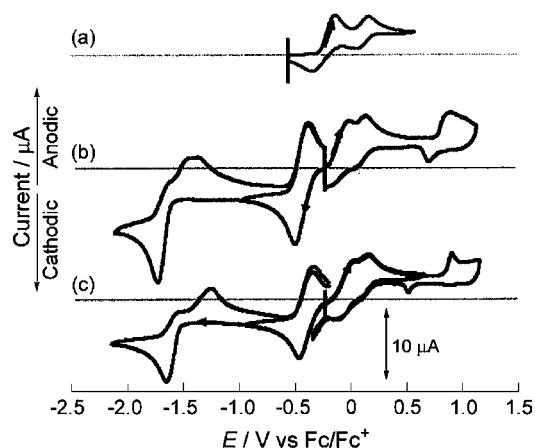


Figure 4. Cyclic voltammograms of (a) tetraethylammonium iodide (TEAI), (b) [CpCo(I)(SSH)] (**2**), and (c) [CpCo(I)(SST)] (**1**) in dichloromethane solution containing TBAP. **1** and **2** generate the iodide-free [CpCo(SST)]⁺ (4^+) and [CpCo(SSH)]⁺ (5^+) complexes in solution.

nium perchlorate (TBAP). Those first reduction waves are reversible, and their reduction potentials appeared at -0.41 V for **1** and -0.45 V for **2** (vs Fc/Fc⁺). Two irreversible oxidation waves around 0 V in both **1** and **2** are probably due to the presence of a naked iodide anion, because the CV of tetraethylammonium iodide (TEAI) also gave similar oxidation waves (Figure 4a). Voltammetric oxidation of iodide reported that the first $2e^-$ oxidation of iodide yields triiodide (I₃⁻), and thus, the second oxidation is due to $1e^-$ oxidation of the generated triiodide.²⁴

1 or **2** precedently releases the iodide anion in solution and then generates coordinatively unsaturated five-coordinate species, [CpCo(SST)]⁺ (4^+) or [CpCo(SSH)]⁺ (5^+), respectively. One important fact is that the reduction potentials of the CpCo–SST and CpCo–SSH complexes appeared at -0.41 and -0.45 V (vs Fc/Fc⁺), which are more positive than those of [CpCo(S₂C₂(CN)₂)] (-0.74 V) and [CpCo(S₂C₂(CO₂Me)₂)] (-1.00 V).¹⁷ The latter two dithiolene complexes are coordinatively unsaturated and some of the most electron-poor [CpCo(dithiolene)] complexes by the electron-withdrawing groups on the dithiolene ligand. If there is a six-coordinate species with no iodide elimination, we do not observe any reduction waves in this potential range. Accordingly, we concluded that **1** and **2** existed as iodide-free 4^+ and 5^+ in solution, respectively. As described above in the synthetic part of this paper, elimination of iodide ligand may be a barrier to isolation of **1** or **2** using column chromatography on silica gel. We assume that a strong electronic donation of the thiolate ligand kicks out the iodide ligand to form 4^+ or 5^+ in solution but electronic electron delocalization in the metalla-cycle (or cobaltadithiaazulene ring) can stabilize the coordinatively unsaturated Co atom, thanks to the redox active SST or SSH ligand. Actually, the calculated LUMO of 4^+ indicates that there is a large contribution of the LUMO at the CpCo moiety, but basically it is delocalized in the whole molecule (Figure 5a). [CpCo(bdt)] also showed delocalization

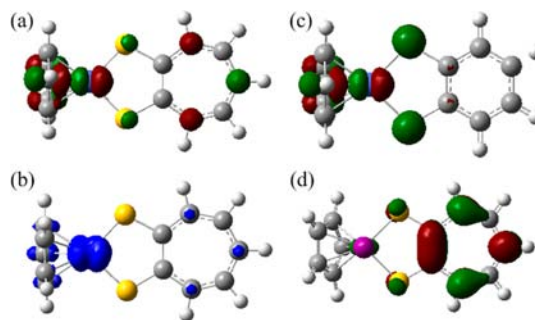


Figure 5. (a) Distribution of the lowest unoccupied molecular orbital (LUMO) of the cation 4^+ , (b) spin density distribution of 4^+ , (c) LUMO of [CpCo(bdt)], and (d) LUMO of **1** (isovalues = 0.05).

of the LUMO (Figure 5c). It is different in that the LUMO of the iodide-coordinated **1** is mostly distributed among the SST ligand but slightly distributed to the CpCo moiety (Figure 5d).

Accordingly, the electron-poor Co atom in 4^+ or 5^+ is probably easily reduced. In fact, the ESR spectrum of the in-situ-generated neutral radical 4^{\bullet} (Figure 6), which was formed by cathodic bulk electrolysis of 4^+ at -0.9 V, indicated eight divided signals by the nuclear spin $7/2$ of a Co atom ($g = 2.08$, $A_{iso} = 3.46$ mT), suggesting a strong contribution of a Co^{II} state. In addition to this experimental evidence, DFT calculation of the neutral radical 4^{\bullet} indicated that there is

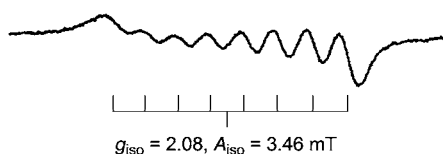


Figure 6. ESR spectrum of the in-situ-generated 4^\bullet obtained by the $1e^-$ reduction of 4^+ at -0.9 V.

97% spin density on the central Co atom, as also described in the spin density distribution of 4^\bullet (Figure 5b). This ESR result of 4^\bullet is almost comparable with those of the $1e^-$ reduced $[\text{CpCo}(\text{dithiolene})]^-$ radical anion species ($g = 2.09\text{--}2.11$).²⁵

We measured UV–vis–NIR spectra of the in-situ-generated neutral radical 4^\bullet under Ar atmosphere using an optically transparent thin-layer electrode (OTTLE) cell. The continual spectral measurement with the electrochemical reduction of 4^+ at -0.9 V for 2 min demonstrated spectral changes with several isosbestic points around 420, 475, 680, and 905 nm (Figure 7a). Two broad peaks around 570 and 800 nm decreased, and peaks at 645 and 450 nm and a broad peak around 1050 nm increased instead. The final spectrum after 2 min reduction is formally corresponding to that of the neutral radical 4^\bullet . The low-energy NIR absorption at 1050 nm is probably due to delocalization of the singly occupied molecular orbital (SOMO) in 4^\bullet such as that in the square-planar $[\text{M}(\text{dithiolene})_2]$ radical anion.²⁶ Furthermore, reoxidation 4^\bullet at -0.3 V for 2 min with the OTTLE showed complete recovery of the original spectrum (Figure 7b). After $1e^-$ reduction at -0.9 V for 30 min and then reoxidation at -0.3 V, we observed the same recovery of the spectrum (not shown). This result revealed that the in-situ-generated cation 4^+ can be reversibly reduced and the neutral species 4^\bullet is stable enough on a time scale of 10 min. In addition to 4^+ , the OTTLE spectra of the in-situ-generated cation 5^+ also gave similar spectral changes and enough stability of the neutral radical 5^\bullet .

On the other hand, the second reduction waves of the in-situ-generated 4^+ ($E_p = -1.65$ V) and 5^+ ($E_p = -1.74$ V) were obviously irreversible (Figure 4b and 4c), indicating the instability of $2e^-$ reduced 4^{2-} and 5^{2-} anion species, respectively. The presence of the second reduction wave is slightly unexpected for us, because the CVs of normal $[\text{CpCo}(\text{dithiolene})]$ complexes have shown a sole reduction wave based on the $\text{Co}^{\text{II}}/\text{Co}^{\text{III}}$ redox couple.²⁷ While comparing the reduction potentials of 4^+ and 5^+ , 5^+ has more negative potentials than that of the other thanks to the electron-donating *i*Pr group on the seven-membered ring. Note that the

difference between these second reduction potentials ($\Delta E_2 = 0.09$ V) is larger than that between the first reduction potentials ($\Delta E_1 = 0.04$ V) in 4^+ vs 5^+ . We assume that the second reduction occurs on the seven-membered ring moiety because the electron-donating *i*Pr group effect the second reduction potential more than that on the first one, indicating generation of an anion radical based on the seven-membered ring.

After the second reduction of 4^+ and 5^+ , the reverse potential scan gave two reoxidation waves around -1.4 V (Figure 4b and 4c). In order to check the details, continual spectral measurements during electrolyses were performed by the OTTLE cell. After the 2 min reduction of the cation 4^+ , the generated neutral 4^\bullet was further reduced at -1.9 V in the OTTLE cell (Figure 8a). The spectral changes did not show any isosbestic points. It is different from measurement of the $4^\bullet/4^+$ process (Figure 7a). This fact means that there is not only electron transfer reaction but also one (or more) chemical reaction(s) at this stage. It is consistent with irreversibility of the second reduction wave in the CVs (Figure 4b and 4c). During the second reduction at -1.9 V, the peaks of the neutral 4^\bullet at 645 and 450 nm decreased. Reoxidation at -0.9 V of the reduced product for 2 min showed a peak at 635 nm (Figure 8b), which is clearly different from the spectrum of 4^\bullet (645 nm). However, the spectra spontaneously changed during 2 min at -0.9 V. The peak at 635 nm slowly shifted to 645 nm. Absorbances at 450 and 1050 nm were further enhanced. The final spectrum after 8 min just became the original spectrum of the neutral 4^\bullet (Figure 8c).

The chemical reduction of azulene with sodium metal was previously performed by Bock et al., and X-ray diffraction study of the isolated product proved the structure of a dimerized azulene, which was formed by an anion radical coupling of the reduced azulene monomer at the 6 position in the seven-membered ring moiety (Scheme 3).²⁸ We calculated the optimized structure of the radical anion of azulene and then revealed that 42% spin density existed at the 6 position in the seven-membered ring. This result theoretically explains that the azulene radical anion can dimerize by a radical coupling mechanism. Similarly, we can assume that the resulted $4^{\bullet-}$ undergoes a dimerization of the cobaltadithiaazulene ring (Scheme 2). The appearance of two reoxidation waves in the CVs can be evidence for the existence of the dimeric complex with an electronic interaction. Unlike the formation mechanism of azulene dimer at the 6 position, we observed large spin densities of 30–32% in the calculated $4^{\bullet-}$ anion at the 5 or 7 position more than that of 16% at the 6 position, namely, the anion radical coupling of $4^{\bullet-}$ occurs at a different position from

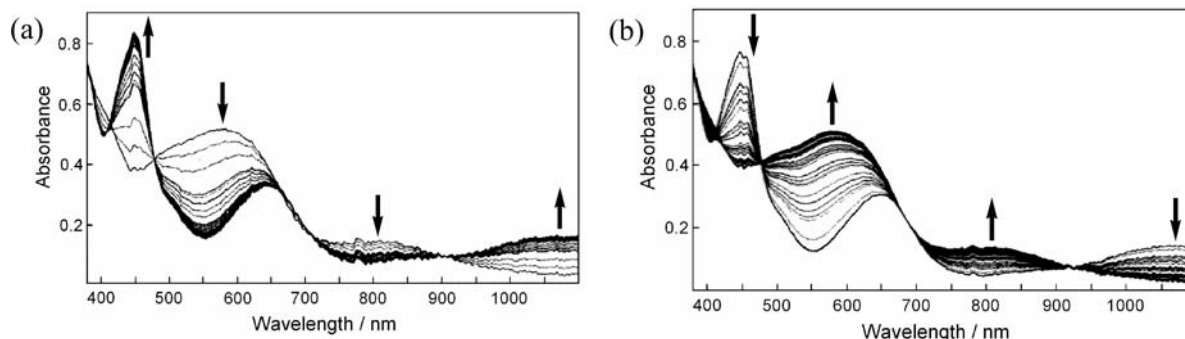


Figure 7. UV–vis–NIR spectral changes of the in-situ-generated cation 4^+ during electrolyses: (a) first reduction at -0.9 V for 2 min and (b) reoxidation at -0.3 V for 2 min.

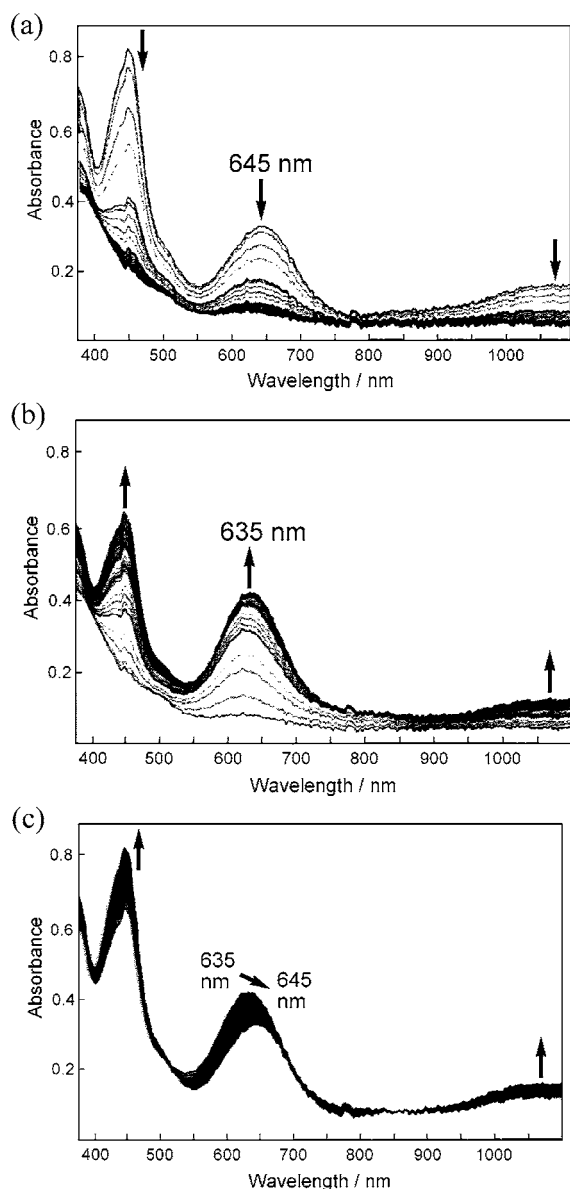


Figure 8. UV-vis-NIR spectral changes of the in-situ-generated neutral 4^* during electrolyses: (a) second reduction at -1.9 V for 2 min, (b) reoxidation at -0.9 V for 2 min, and (c) retention at -0.9 V for 6 min.

a normal azulene (Schemes 2 and 3). We believe that our result is the first case of the reductive-dimerization of a metal-laheteroazulene compound. Furthermore, the spectral changes from 635 to 645 nm upon reoxidation of the proposed dianionic dimer 6^{2-} supported that the neutral dimer **6** slowly becomes the original monomer 4^* . Eventually, we can reversibly and electrochemically control the dimer-monomer structural changes of the cobaltadithiaazulene complex by ECEC reactions. Therefore, the redox behavior between **4** and **6** can be described as an electrochemical square scheme (Scheme 2).²⁹

CONCLUSION

We reported the simple and straightforward preparation of the SST or SSH derivative from tropolone or hinokitiol by a single-step reaction, although previous work by another research group required three-step reactions.⁴ Furthermore, $[\text{CpCo}(\text{I})$ -

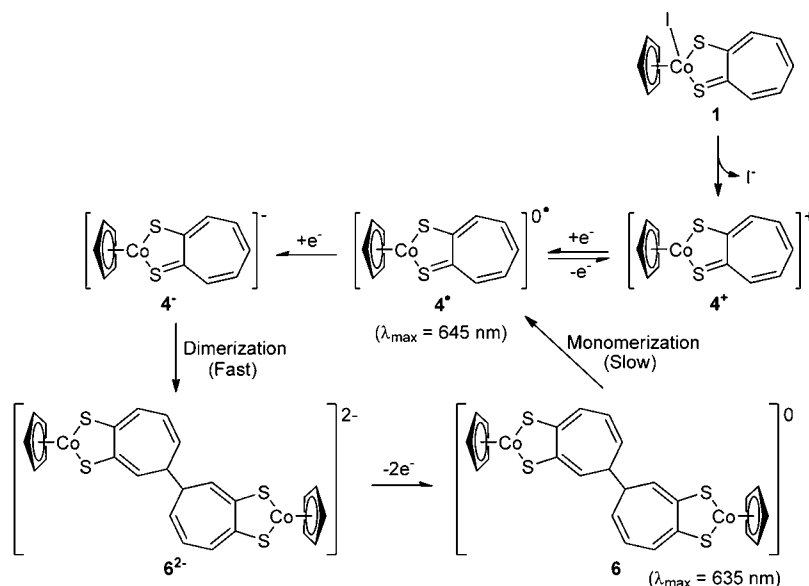
(SST)] (**1**) and $[\text{CpCo}(\text{I})(\text{SSH})]$ (**2**) complexes are new products as organometallic SST metal complexes. **1** and **2** include cobaltadithiaazulene rings with a formal 10π -electron conjugation, because there is a π -conjugated metallacycle with a cycloheptatriene backbone. Electrochemical studies of **1** and **2** clarified the generation of those iodide-free complexes (4^+ and 5^+) in solutions and novel reductive-dimerization of the cobaltadithiaazulene ring. This dimerization is due to the uniqueness of the electron-poor seven-membered ring. The DFT study on 4^+ or 4^* indicated delocalization of the LUMO or SOMO in the whole molecule; thus, $[\text{CpCo}(\text{SST})]$ enters into the π -delocalized organometallic system including a Cp ligand orbital. In these CpCo-SST (or SSH) complexes, there could be metal/ligand electron transfer since the SST (or SSH) ligand is potentially redox active. Currently, we are trying to isolate the coordinatively unsaturated 4^+ and 5^+ species using soft anions (BF_4^- , PF_6^- , NO_3^- , and so on) instead of iodide. Those catalytic activities and small molecule activations may be observed as similar to the cases of the coordinatively unsaturated $[\text{CpCo}(\text{dithiolene})]$ complexes.³⁰ Furthermore, one will be able to synthesize other organometallic ($\eta^5\text{-C}_5\text{R}_5$)M complexes ($\eta^5\text{-C}_5\text{R}_5 = \text{Cp}$ and Cp^* ; M = Rh, Ir, and Ni) and other six-coordinate complexes (M = 5–6 group metals) of the SST or SSH ligand using our straightforward synthetic procedure.

EXPERIMENTAL SECTION

Materials and Instrumentation. All reactions were carried out under an argon atmosphere by means of standard Schlenk techniques. 1,4-Dioxane was obtained from Wako Pure Chemical Industries, Ltd. and then distilled by Na-benzophenone before use. CH_2Cl_2 and MeOH (Wako) were dried with CaH_2 before use. Tropolone, phosphorus pentasulfide (P_2S_5), and silica gel (Wakogel C-300) were obtained from Wako Pure Chemical Industries, Ltd. Hinokitiol and Lawesson's reagent were obtained from Tokyo Chemical Industries, Co., Ltd. $[\text{CpCoI}_2(\text{CO})]$ was prepared by a known procedure.³¹ Elemental analyses were determined using a Shimadzu PE2400-II instrument. The mass spectrum was recorded on a JEOL JMS-D300. NMR spectra were measured with a JEOL LA500 spectrometer. UV-vis spectra were recorded on a Hitachi model UV-2500PC.

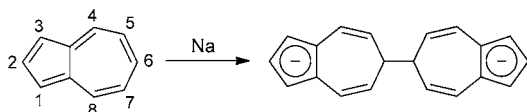
Preparation of $[\text{PS}_2(\text{SST})]_2$ and $[\text{PS}_2(\text{SSH})]_2$. Tropolone (2.44 g, 20 mmol) and P_2S_5 (8.88 g, 40 mmol) were reacted in refluxing 1,4-dioxane solution (70 mL) for 3 h. The initial yellow suspension changed to a red suspension. After cooling the solution at room temperature, the red suspension was filtered and the resulting red solids were further washed with hot 1,4-dioxane. The red solids were dried under vacuum, and then $[\text{PS}_2(\text{SST})]_2$ was obtained in 87% yield. $[\text{PS}_2(\text{SSH})]_2$ was also prepared by a similar procedure to that of the SST derivative from hinokitiol.

Preparation of $[\text{CpCo}(\text{I})(\text{SST})]$ (1**) and $[\text{CpCo}(\text{I})(\text{SSH})]$ (**2**).** $[\text{CpCoI}_2(\text{CO})]$ (0.487 g, 1.20 mmol) was reacted with $[\text{PS}_2(\text{SST})]_2$ (0.298 g, 0.60 mmol) in CH_2Cl_2 (30 mL)/MeOH (10 mL) solution at room temperature. After stirring for 16 h, some black solids were precipitated. The black solids were collected by filtration and then washed with MeOH. At this stage, the obtained filtrate contains $[\text{CpCo}(\text{I})(\text{S}_2\text{P}(\text{OMe})_2)]$ (**3**). On the other hand, the resulting black solids were dissolved into a minimum amount of dichloromethane and then filtered to remove some insoluble components. *n*-Hexane was added into the resulting filtrate, and then the product was recrystallized by slow evaporation. $[\text{CpCo}(\text{I})(\text{SST})]$ (**1**) was obtained in 28% yield. A dark green fraction of **3** was separated by column chromatography on silica gel (54% yield). The corresponding SSH derivative $[\text{CpCo}(\text{I})(\text{SSH})]$ (**2**) was prepared from $[\text{CpCoI}_2(\text{CO})]$ (0.247 g, 0.609 mmol) and $[\text{PS}_2(\text{SSH})]_2$ (0.174 g, 0.30 mmol) using a similar procedure to that of **1**. **2** and **3** were isolated in 44% and 20% yields, respectively.

Scheme 2. Proposed Electrochemical (E) and Chemical Reaction (C) Schemes of 4^n ($n = -1, 0, +1$)^a

^aE reactions are right and left. C reactions are up and down.

Scheme 3. Reductive–Dimerization of Azulene at the 6 Position

Table 2. Crystal Data^a

	1
formula	C ₁₂ H ₁₀ CoIS ₂
fw (g·mol ⁻¹)	404.17
cryst color	black
cryst shape	platelet
cryst size (mm)	0.30 × 0.15 × 0.05
cryst syst	triclinic
space group	P-1 (No. 2)
T (K)	298
a (Å)	8.005(2)
b (Å)	12.947(3)
c (Å)	13.814(4)
α (deg)	73.162(11)
β (deg)	75.546(11)
γ (deg)	73.341(11)
V (Å ³)	1291.0(6)
Z	4
D _{calcd} (g·cm ⁻³)	2.079
μ (mm ⁻¹)	4.013
total reflns	10 074
unique reflns (R _{int})	5651 (0.037)
unique reflns (I > 2σ(I))	4264
R ₁ (I > 2σ(I))	0.0349
wR ₂ (I > 2σ(I))	0.0928
goodness-of-fit	1.038

$$^a R_1 = \frac{\sum ||F_o| - |F_c||}{\sum |F_o|}; wR_2 = \frac{[\sum (w(F_o^2 - F_c^2)^2)]^{1/2}}{[\sum w(F_o^2)^2]^{1/2}}$$

Spectroscopic Data of 1. Mass (EI⁺, 1.3 kV) *m/z* (rel intensity) 277 (M⁺ - I, 100), 254 (I₂, 59), 212 (M⁺ - CpI, 49), 153 (S₂C₇H₅⁺, 15), 121 (SC₇H₅⁺, 15), 59 (Co⁺, 27). ¹H NMR (CDCl₃, vs TMS, 500

MHz) δ 7.58 (d, 2H, *J* = 11.0 Hz, C₇H₅ ring), 6.77 (t, 2H, *J* = 11.0 Hz, C₇H₅ ring), 6.55 (t, 1H, *J* = 11.0 Hz, C₇H₅ ring), 5.32 (s, 5H, Cp). UV-vis (CH₂Cl₂) λ_{max}/nm (ε/M⁻¹·cm⁻¹) 588 (4100), 288 (21 000). Anal. Calcd for C₁₂H₁₀CoIS₂: C, 35.66; H, 2.49. Found: C, 35.70; H, 2.55.

Spectroscopic Data of 2. Mass (EI⁺, 1.3 kV) *m/z* (rel intensity) 319 (M⁺ - I, 100), 304 (M⁺ - MeI, 100), 254 (I₂, 63), 238 (M⁺ - CpMeHI, 29), 127 (I⁺, 24), 59 (Co⁺, 29). ¹H NMR (CDCl₃, vs TMS, 500 MHz) δ 7.64 (s, 1H, C₇H₄ ring), 7.52 (d, 1H, *J* = 11.8 Hz, C₇H₄ ring), 6.75 (t, 1H, *J* = 10.4 Hz, C₇H₄ ring), 6.50 (d, 1H, *J* = 9.9 Hz, C₇H₄ ring), 5.30 (s, 5H, Cp), 2.57 (sp, 1H, *J* = 6.8 Hz, CHMe₂), 1.17 (d, 6H, *J* = 6.8 Hz, CHMe₂). UV-vis (CH₂Cl₂) λ_{max}/nm (ε/M⁻¹·cm⁻¹) 588 (4500), 289 (22 000). Anal. Calcd for C₁₅H₁₆CoIS₂: C, 40.37; H, 3.61. Found: C, 40.44; H, 3.68.

Spectroscopic Data of 3. Mass (EI⁺, 1.3 kV) *m/z* (rel intensity) 281 (M⁺ - I, 85), 254 (I₂, 21), 216 (M⁺ - CpI, 17), 93 (P(OMe)₂⁺, 100). ¹H NMR (CDCl₃, vs TMS, 500 MHz) δ 5.40 (s, 5H, Cp), 3.67 (d, 3H, *J*_{P-H} = 14.0 Hz, OMe), 3.43 (d, 3H, *J*_{P-H} = 15.0 Hz, OMe). Anal. Calcd for C₇H₁₁CoIO₂PS₂: C, 20.60; H, 2.72. Found: C, 20.78; H, 2.99.

CV Measurements. All electrochemical measurements were performed under an argon atmosphere. Solvents for electrochemical measurements were dried by molecular sieve 4A before use. A platinum wire served as a counter electrode, and the reference electrode Ag/AgCl was corrected for junction potentials by being referenced internally to the ferrocene/ferrocenium (Fc/Fc⁺) couple. A stationary platinum disk (1.6 mm in diameter) was used as a working electrode. The model CV-50W instrument from BAS Co. was used for cyclic voltammetry (CV) measurements. CVs were measured in 1 mmol·dm⁻³ dichloromethane solutions of complexes containing 0.1 mol·dm⁻³ tetra-*n*-butylammonium perchlorate (TBAP) at 25 °C.

Spectroelectrochemical Measurement. UV-vis-NIR absorption spectra were obtained during electrolysis for 1 mmol·dm⁻³ dichloromethane solutions of complexes containing 0.1 mol·dm⁻³ TBAP at 25 °C in an optically transparent thin-layer electrode (OTTLE, thin-layer thickness = 0.4 mm)³² cell. Measurements were made with a MCPD-7000 rapid scan spectrometer and MC-2530 of Otsuka Electronics Co., Ltd. The working electrode was a stationary platinum mesh in thin-layer form.

Density Functional theory (DFT) Calculation. Geometries of [CpCo(SST)]ⁿ (4ⁿ, *n* = -1, 0, +1), free SSTⁿ ligand (*n* = -1, 0, +1), [CpCo(bdt)]ⁿ (*n* = -1, 0), and azulene radical anion were optimized with no constraint using the Gaussian 03 package³³ and the hybrid

functional B3LYP for closed-shell molecules or UB3LYP for open-shell molecules.³⁴ For [CpCo(SST)]ⁿ and [CpCo(bdt)]ⁿ, the standard 6-31G* basis³⁵ set was used for H, C, and S together with the LanL2DZ for Co. Energy minima were confirmed by frequency analysis.

X-ray Diffraction Study. A single crystal of **1** was obtained by recrystallization using vapor diffusion of *n*-hexane into the dichloromethane solution. It was mounted on top of a thin glass fiber. Measurement was made on a Rigaku Mercury diffractometer with graphite-monochromated Mo K α radiation. Data were corrected for Lorentz and polarization effects. The structure was solved by direct methods and expanded using Fourier techniques.³⁶ Non-hydrogen atoms were refined anisotropically. Hydrogen atoms were refined using the riding model. All calculations were carried out using the Crystal Structure crystallographic software package.³⁷ Crystallographic data are summarized in Table 2.

■ ASSOCIATED CONTENT

● Supporting Information

Structure of [CpCo(I)(SST)] (**1**) in CIF format. This material is available free of charge via the Internet at <http://pubs.acs.org>.

■ AUTHOR INFORMATION

Corresponding Author

*E-mail: mitsushiro@riken.jp (M.N.); kajita-m@sophia.ac.jp (M.K.).

Present Addresses

[†]Condensed Molecular Materials Laboratory, RIKEN, 2-1, Hirosawa, Wako-shi, Saitama 351-0198, Japan.

[‡]School of Public Health, Department of Epidemiology, Harvard University, 677 Huntington Avenue, Kresge 913, Boston, Massachusetts 02115, United States.

Notes

The authors declare no competing financial interest.

■ ACKNOWLEDGMENTS

We thank Dr. Kusamoto (University of Tokyo) for helpful discussion about DFT calculations.

■ REFERENCES

- (1) Liu, R. S. H.; Asato, A. E. *J. Photochem. Photobiol. C, Photochem. Rev.* **2003**, *4*, 179.
- (2) (a) Hahn, F. E.; Jahnke, M. C. *Angew. Chem., Int. Ed.* **2008**, *47*, 3122. (b) Tanaka, Y.; Mitani, A.; Igarashi, T.; Someya, S.; Otsuka, K.; Imai, T.; Yamaki, F.; Tanaka, H.; Saitoh, M.; Nakazawa, T.; Noguchi, K.; Hashimoto, K.; Shigenobu, K. *Naunyn Schmiedebergs Arch. Pharmacol.* **2001**, *363*, 344.
- (3) (a) Hahn, F. E.; Wittenbecher, L.; Boese, R.; Bläser, D. *Chem.—Eur. J.* **1999**, *5*, 1931. (b) Hahn, F. E.; Wittenbecher, L.; Van, D. L.; Fröhlich, R. *Angew. Chem., Int. Ed.* **2000**, *39*, 541. (c) Hahn, F. E.; Foth, M. *J. Organomet. Chem.* **1999**, *585*, 241.
- (4) (a) Forbes, C. E.; Holm, R. H. *J. Am. Chem. Soc.* **1968**, *90*, 6884. (b) Forbes, C. E.; Holm, R. H. *J. Am. Chem. Soc.* **1970**, *92*, 2297. (c) Herskovitz, T.; Forbes, C. E.; Holm, R. H. *Inorg. Chem.* **1972**, *11*, 1318.
- (5) (a) Wang, K. *Prog. Inorg. Chem.* **2003**, *52*, 267. (b) Nomura, M.; Fujita-Takayama, C.; Sugiyama, T.; Kajitani, M. *J. Organomet. Chem.* **2011**, *696*, 4018.
- (6) (a) Cummings, S. D.; Eisenberg, R. *Prog. Inorg. Chem.* **2003**, *52*, 315. (b) Paw, W.; Cummings, S. D.; Mansour, M. A.; Connick, W. B.; Geiger, D. K.; Eisenberg, R. *Coord. Chem. Rev.* **1998**, *171*, 125.
- (7) (a) Faulmann, C.; Cassoux, P. *Prog. Inorg. Chem.* **2003**, *52*, 399. (b) Kato, R. *Chem. Rev.* **2004**, *104*, 5319.
- (8) Kreckmann, T.; Hahn, F. E. *Chem. Commun.* **2007**, 1111.
- (9) Eisenberg, R.; Khare, G. P.; Schultz, A. J. *J. Am. Chem. Soc.* **1971**, *93*, 3597.

(10) (a) Sun, G.-X.; Kakei, C.; Kume, E.; Hatsui, T.; Ujiie, S.; Mori, A. *Liq. Cryst.* **2007**, *34*, 927. (b) Chipperfield, J. R.; Clark, S.; Elliott, J.; Sinn, E. *Chem. Commun.* **1998**, 195.

(11) (a) Kunkely, H.; Pawlowski, V.; Vogler, A. Z.; Naturforsch., B J. *Chem. Sci.* **2008**, *63*, 963. (b) Takagi, K.; Saiki, K.; Hayashi, H.; Ohsawa, H.; Matsuoka, S.; Suzuki, M. *Bull. Chem. Soc. Jpn.* **2009**, *82*, 236. (c) Zhang, J.; Badger, P. D.; Geib, S. J.; Petoud, S. *Inorg. Chem.* **2007**, *46*, 6473.

(12) Bhalla, G.; Periana, R. A. *Angew. Chem., Int. Ed.* **2005**, *44*, 1540.

(13) (a) Camard, A.; Ihara, Y.; Murata, F.; Mereiter, K.; Fukuda, Y.; Linert, W. *Inorg. Chim. Acta* **2005**, *358*, 409. (b) Ihara, Y.; Yoshizakiya, M.; Yoshiyama, R.; Sone, K. *Polyhedron* **1996**, *15*, 3643.

(14) (a) Rauchfuss, T. B. *Prog. Inorg. Chem.* **2003**, *52*, 1. (b) Schrauzer, G. N.; Meyweg, V. P. *J. Am. Chem. Soc.* **1965**, *87*, 1483.

(15) Lecher, H. Z.; Greenwood, R. A.; Whitehouse, K. C.; Chao, T. H. *J. Am. Chem. Soc.* **1956**, *78*, 5018.

(16) Cullen, E. P.; Doherty, J.; Manning, A. R.; McArdle, P.; Cunningham, D. *J. Organomet. Chem.* **1988**, *348*, 109.

(17) Nomura, M. *Dalton Trans.* **2011**, *40*, 2112.

(18) Sellmann, D.; Geck, M.; Knoch, F.; Ritter, G.; Dengler, J. *J. Am. Chem. Soc.* **1991**, *113*, 3819.

(19) Nomura, M.; Sasao, T.; Hashimoto, T.; Sugiyama, T.; Kajitani, M. *Inorg. Chim. Acta* **2010**, *363*, 3647.

(20) Fourmigué, M.; Cauchy, T.; Nomura, M. *CrystEngComm* **2009**, *11*, 1491.

(21) Reinheimer, E. W.; Olejniczak, I.; Łapiński, A.; Świetlik, R.; Jeannin, O.; Fourmigué, M. *Inorg. Chem.* **2010**, *49*, 9777.

(22) [CpCo(bdt)] is a monomer at 150 °C in the crystal but dimerizes at room temperature, see: Miller, E. J.; Brill, T. B.; Rheingold, A. L.; Fultz, W. C. *J. Am. Chem. Soc.* **1983**, *105*, 7580.

(23) Chaudhuri, P.; Verani, C. N.; Bill, E.; Bothe, E.; Weyhermüller, T.; Wieghardt, K. *J. Am. Chem. Soc.* **2001**, *123*, 2213.

(24) Zhang, Y.; Zheng, J. B. *Electrochim. Acta* **2007**, *52*, 4082.

(25) (a) Nomura, M.; Kanamori, M.; Tateno, N.; Fujita-Takayama, C.; Sugiyama, T.; Kajitani, M. *J. Organomet. Chem.* **2010**, *695*, 2432. (b) Takayama, C.; Takeuchi, K.; Ohkoshi, S.; Kajitani, M.; Sugimori, A. *Organometallics* **1999**, *18*, 4032.

(26) (a) Kirk, M. L.; McNaughton, R. L.; Helton, M. E. *Prog. Inorg. Chem.* **2003**, *52*, 111. (b) Faulmann, C.; Cassoux, P. *Prog. Inorg. Chem.* **2003**, *52*, 399.

(27) Nomura, M.; Kondo, S.; Yamashita, S.; Suzuki, E.; Toyota, Y.; Alea, G. V.; Janairo, G. C.; Fujita-Takayama, C.; Sugiyama, T.; Kajitani, M. *J. Organomet. Chem.* **2010**, *695*, 2366.

(28) Bock, H.; Arad, C.; Naether, C.; Goebel, I. *Helv. Chim. Acta* **1996**, *79*, 92.

(29) (a) Richards, T. C.; Geiger, W. E. *J. Am. Chem. Soc.* **1994**, *116*, 2028. (b) Connelly, N. G.; Geiger, W. E.; Lagunas, M. C.; Metz, B.; Rieger, A. L.; Rieger, P. H.; Shaw, M. J. *J. Am. Chem. Soc.* **1995**, *117*, 12202.

(30) (a) Nomura, M.; Hatano, H.; Fujita, T.; Eguchi, Y.; Abe, R.; Yokoyama, M.; Takayama, C.; Akiyama, T.; Sugimori, A.; Kajitani, M. *J. Organomet. Chem.* **2004**, *689*, 993. (b) Sugimori, A.; Kajitani, M. *Kagaku Zokan* **1988**, *115*, 113.

(31) King, R. B. *Inorg. Chem.* **1966**, *5*, 82.

(32) (a) Ushijima, H.; Sudoh, S.; Kajitani, M.; Shimizu, K.; Akiyama, T.; Sugimori, A. *Appl. Organomet. Chem.* **1991**, *5*, 221. (b) Shimizu, K.; Ikehara, H.; Kajitani, M.; Ushijima, H.; Akiyama, T.; Sugimori, A.; Satō, G. P. *J. Electroanal. Chem.* **1995**, *396*, 465.

(33) Frisch, M. J.; Trucks, G. W.; Schlegel, H. B.; Scuseria, G. E.; Robb, M. A.; Cheeseman, J. R.; Montgomery, J. A., Jr.; Vreven, T.; Kudin, K. N.; Burant, J. C.; Millam, J. M.; Iyengar, S. S.; Tomasi, J.; Barone, V.; Mennucci, B.; Cossi, M.; Scalmani, G.; Rega, N.; Petersson, G. A.; Nakatsuji, H.; Hada, M.; Ehara, M.; Toyota, K.; Fukuda, R.; Hasegawa, J.; Ishida, M.; Nakajima, T.; Honda, Y.; Kitao, O.; Nakai, H.; Klene, M.; Li, X.; Knox, J. E.; Hratchian, H. P.; Cross, J. B.; Adamo, C.; Jaramillo, J.; Gomperts, R.; Stratmann, R. E.; Yazyev, O.; Austin, A. J.; Cammi, R.; Pomelli, C.; Ochterski, J. W.; Ayala, P. Y.; Morokuma, K.; Voth, G. A.; Salvador, P.; Dannenberg, J. J.; Zakrzewski, V. G.; Dapprich, S.; Daniels, A. D.; Strain, M. C.;

Farkas, O.; Malick, D. K.; Rabuck, A. D.; Raghavachari, K.; Foresman, J. B. Ortiz, J. V.; Cui, Q.; Baboul, A. G.; Clifford, S.; Cioslowski, J.; Stefanov, B. B.; Liu, G.; Liashenko, A.; Piskorz, P.; Komaromi, L.; Martin, R. L.; Fox, D. J.; Keith, T.; Al-Laham, M. A.; Peng, C. Y.; Nanayakkara, A.; Challacombe, M.; Gill, P. M. W.; Johnson, B.; Chen, W.; Wong, M. W.; Gonzalez, C.; Pople, J. A. *Gaussian 03*, revision B.03; Gaussian, Inc.: Pittsburgh, PA, 2003.

(34) (a) Becke, A. D. *J. Chem. Phys.* **1986**, *84*, 4524. (b) Becke, A. D. *J. Chem. Phys.* **1993**, *98*, 5648. (c) Lee, C. T.; Yang, W. T.; Parr, R. G. *Phys. Rev. B* **1988**, *37*, 785.

(35) (a) Krishnan, R.; Binkley, J. S.; Seeger, R.; Pople, J. A. *J. Chem. Phys.* **1980**, *72*, 650. (b) Blaudau, J.-P.; McGrath, M. P.; Curtiss, L. A.; Radom, L. *J. Chem. Phys.* **1997**, *107*, 5016. (c) Curtiss, L. A.; McGrath, M. P.; Blandeau, J.-P.; Davis, N. E.; Binning, R. C., Jr.; Radom, L. *J. Chem. Phys.* **1995**, *103*, 6104.

(36) Beurstkens, P. T.; Admiraal, G.; Beurskens, G.; Bosman, W. P.; Garcia-Granda, S.; Gould, R. O.; Smits, J. M. M.; Smykala, C. The DIRDIF Program System. *Technical Report of the Crystallography Laboratory*; University of Nijmegen: Nijmegen, The Netherlands, 1992.

(37) *Crystal Structure 3.6.0, Single Crystal Structure Analysis Software*; Molecular Structure Corp. and Rigaku Corp.: The Woodlands, TX/Tokyo, Japan, 2004.